



**HAL**  
open science

## Iontophoresis of treprostinil promotes wound healing in a murine model of scleroderma-related ulcers

Sylvain Kotzki, Yann Savina, Raphael Bouvet, Hugo Gil, Sophie Blaise,  
Jean-Luc Cracowski, Matthieu Roustit

### ► To cite this version:

Sylvain Kotzki, Yann Savina, Raphael Bouvet, Hugo Gil, Sophie Blaise, et al.. Iontophoresis of treprostinil promotes wound healing in a murine model of scleroderma-related ulcers. *Rheumatology*, 2022, 61 (6), pp.2704-2708. 10.1093/rheumatology/keab852 . hal-04445911

**HAL Id: hal-04445911**

**<https://hal.science/hal-04445911v1>**

Submitted on 8 Feb 2024

**HAL** is a multi-disciplinary open access archive for the deposit and dissemination of scientific research documents, whether they are published or not. The documents may come from teaching and research institutions in France or abroad, or from public or private research centers.

L'archive ouverte pluridisciplinaire **HAL**, est destinée au dépôt et à la diffusion de documents scientifiques de niveau recherche, publiés ou non, émanant des établissements d'enseignement et de recherche français ou étrangers, des laboratoires publics ou privés.



Distributed under a Creative Commons Attribution - NonCommercial - NoDerivatives 4.0 International License

**Iontophoresis of treprostinil promotes wound healing in a murine model of scleroderma-related ulcers**

|   |  |
|---|--|
| Journal:  | <i>Rheumatology</i>  |
| Manuscript ID   | Draft  |
| Manuscript Type:  | Concise Report   |
| Date Submitted by the Author:   | n/a  |
| Complete List of Authors:   | KOTZKI, Sylvain; Univ. Grenoble Alpes, Inserm, UMR1300, HP2; Grenoble-Alpes University Hospital, -<br>SAVINA, Yann; Univ. Grenoble Alpes, Inserm, UMR1300, HP2<br>BOUVET, Raphael; Univ. Grenoble Alpes, Inserm, UMR1300, HP2<br>GIL, Hugo; Grenoble-Alpes University Hospital, -<br>blaise, sophie; Univ. Grenoble Alpes, Inserm, UMR1300, HP2; Grenoble-Alpes University Hospital, -<br>Cracowski, Jean-Luc; Univ. Grenoble Alpes, Inserm, UMR1300, HP2; Grenoble-Alpes University Hospital, -<br>Roustit, Matthieu; Univ. Grenoble Alpes, Inserm, UMR1300, HP2; Grenoble-Alpes University Hospital, - |
| Keywords<br>Please select a minimum FIVE keywords from the list provided. These keywords will be used to select reviewers for this manuscript. The keywords in the main text of your paper do not need to match these words.: | Scleroderma and related disorders < RHEUMATIC DISEASES, Animal models < BASIC & CLINICAL SCIENCES, Skin < TISSUES, Drug Design < BASIC & CLINICAL SCIENCES, Pharmacology < BASIC & CLINICAL SCIENCES   |
|   |  |

1 **Iontophoresis of treprostinil promotes wound healing in a murine model of**  
2 **scleroderma-related ulcers.**  
3  
4

5 Sylvain KOTZKI<sup>1,2\*</sup>, Yann SAVINA<sup>1\*</sup>, Raphael BOUVET<sup>1</sup>, Hugo GIL<sup>2</sup>, Sophie BLAISE<sup>1,2</sup>, Jean-  
6 Luc CRACOWSKI<sup>1,2</sup>, Matthieu ROUSTIT<sup>1,2</sup>  
7  
8  
9

10  
11  
12  
13  
14 1 .Univ. Grenoble Alpes, Inserm, UMR1300, HP2, 38000 Grenoble, France  
15

16  
17 2. Grenoble-Alpes University Hospital, 38043 Grenoble, France  
18  
19

20  
21  
22  
23  
24  
25  
26  
27  
28 \*equally contributed to this work  
29

30  
31 Corresponding author:  
32

33  
34 Matthieu Roustit, Unité de Pharmacologie Clinique, Centre d'Investigation Clinique de  
35 Grenoble - Inserm CIC1406, CHU de Grenoble, 38043 Grenoble Cedex 09, France  
36  
37

38  
39 Tel +33 4 76 76 92 60  
40

41  
42 Fax +33 4 76 76 92 62  
43

44  
45 E-mail: [MRoustit@chu-grenoble.fr](mailto:MRoustit@chu-grenoble.fr)  
46

47  
48 Keywords: Scleroderma and related disorders, Pharmacology, Drug design, Skin, Animal  
49 models  
50  
51  
52  
53  
54  
55  
56  
57  
58  
59  
60

**ABSTRACT**

1  
2  
3  
4  
5 **Objective.** Systemic Sclerosis (SSc) is a rare, chronic disease characterized by fibrosis,  
6 vascular alterations and digital ulcerations. Few drugs have shown efficacy to enhance wound  
7 healing of existing SSc-related ulcers. Local delivery of treprostinil, a prostacyclin analogue,  
8 may improve wound healing. The present work aimed, in a first part, at developing a mouse  
9 model of SSc-related ulcerations and, in a second part, at assessing the effect of iontophoresis  
10 of treprostinil on wound healing.  
11  
12  
13  
14  
15

16 **Methods.** We used two murine models of SSc: chemically-induced with HOCl, and Urokinase-  
17 type plasminogen activator receptor (uPAR)-deficient. Excisional wounding was performed on  
18 the dorsal midline with a biopsy punch. Animals were randomized into three groups: treated  
19 with electrostimulation alone, with treprostinil iontophoresis, or untreated. We assessed wound  
20 healing over time, as well as skin microvascular reactivity, inflammation, microvessel density,  
21 and collagen distribution, before wounding and after re-epithelialization.  
22  
23  
24  
25  
26  
27

28 **Results.** uPAR<sup>-/-</sup> mice, but not HOCl-treated mice, showed impaired wound healing and  
29 decreased microvascular reactivity compared with their controls. Treprostinil iontophoresis  
30 improved wound healing and microvascular density and decreased inflammation in uPAR<sup>-/-</sup>  
31 mice, while electro-stimulation did not. However, treprostinil had not effect on microvascular  
32 reactivity and collagen distribution.  
33  
34  
35  
36  
37

38 **Conclusion.** This study suggests that excisional wounds in uPAR<sup>-/-</sup> mice are a relevant model of  
39 SSc-related ulcers. In addition, treprostinil iontophoresis enhances wound healing in this model.  
40 Further work is now needed to show whether this effect translates in humans.  
41  
42  
43  
44  
45  
46  
47  
48  
49  
50  
51  
52  
53  
54  
55  
56  
57  
58  
59  
60

## INTRODUCTION

Systemic Sclerosis (SSc) is a rare, chronic disease characterized by fibrosis, autoimmune abnormalities and vascular alterations, the latter leading to Raynaud's phenomenon and digital ulcerations (DUs). DUs affect about 30% of SSc patients each year, and complications include pain, functional impairment, gangrene and amputations, with a major negative impact on the quality of life [1].

To date, intravenous iloprost, a prostacyclin (PGI<sub>2</sub>) analogue, is the only recommended treatment for active SSc-related DUs [2]. However, its benefit is counterbalanced by dose-limiting, vasodilatation-induced side effects. These safety issues require hospitalization and close monitoring, which increase costs. The paradox is that impaired digital microvasculature in SSc prevents the drug, when administered intravenously, from diffusing properly to the wounded area.

Local treatment may be proposed to get around this issue. We previously demonstrated that digital iontophoresis, a noninvasive, current-driven drug delivery method, could be used to administer treprostinil, another PGI<sub>2</sub> analogue, into the skin of rodents, healthy subjects and SSc patients, leading to a significant increase in skin perfusion [3,4]. This original approach takes advantage of a synergic effect between the pharmacological response to the PGI<sub>2</sub> analogue and the healing properties of electric current. Indeed, electrical current within the wound is known to play a role in healing, by increasing the directed migration of keratinocytes, fibroblasts and neutrophils[5], and has a positive impact on wound healing [6]. Recently, we have further shown that this approach was safe when applied on DUs of patients with SSc [7].

However, whether iontophoresis of treprostinil enhances healing of SSc-related ulcers has never been demonstrated. Experimental data are required to establish the proof-of-concept before moving on to phase 2, clinical studies. The present study aimed at developing a mouse model of SSc-related ulcerations, and at assessing the efficacy of iontophoresis of treprostinil on wound healing.

## METHODS

### *Animals and study design*

The study followed a pre-specified protocol and all procedures were approved by our local institutional review committee (APAFIS#6666-2016031415341059v7) and conducted in accordance with the National Institutes of Health (NIH) Guide for the Care and Use of Laboratory Animals.

1 We used two murine models of SSc and their respective control: a chemically-induced  
2 model (HOCl), and a genetic model (uPAR<sup>-/-</sup>). Animals in the HOCl group received intradermal  
3 injections of of hypochlorous acid (HOCl) to generate oxidative stress during 6 weeks, as  
4 previously described[8]. The control group received injections of sterilized phosphate buffered  
5 saline (PBS) solution following the same protocol. The Urokinase-type Plasminogen Activator  
6 Receptor gene (uPAR<sup>-/-</sup>) mouse model mimics the vascular and fibrotic features of SSc[9].  
7 uPAR<sup>-/-</sup> mice were crossed with wild-type (uPAR<sup>+/+</sup>) mice on a C57BL/6J background to  
8 generate heterozygous uPAR<sup>+/-</sup> mice. The latter were subsequently crossed to generate uPAR<sup>-  
9 /-</sup> and their uPAR<sup>+/+</sup> littermates as controls. Details about animal models are available as online  
10 supplementary methods.  
11  
12  
13  
14  
15  
16  
17  
18

19 Mice were acclimated to the photoperiod (12-hour light/12-hour dark) and temperature  
20 conditions (22±1°C) for one week prior to the start of the study, with food and water ad libitum.  
21  
22  
23

### 24 *Wounding procedure*

25 Mice were anesthetized with isoflurane and analgesia was induced with buprenorphin.  
26 Full-thickness skin excision wound extending through the *panniculus carnosus* was performed  
27 on the dorsal midline. Detailed procedure are available as online supplementary methods.  
28  
29  
30  
31  
32  
33

### 34 *Treprostinil iontophoresis*

35 Treprostinil solution was prepared from a commercial solution at 2.5 mg /mL (6.4 mM)  
36 (Remodulin®, Bioprojet Pharma, Paris, France), 10 times diluted with isotonic sodium chloride  
37 (NaCl 0.9%) (Aguettant, Lyon, France) to obtain a 250 µg/mL (0.64 mM) solution. Mice in  
38 control groups received a solution of NaCl 0.9% (vehicle).  
39  
40  
41  
42  
43

44 To assess a possible impact of sex in our model, the experiment was applied on both  
45 male and female animals. Thus, each sex-group was randomized into three sub-groups,  
46 according to the treatment to be administered: untreated wound, electrostimulation (ES) alone  
47 (current + vehicle), treprostinil iontophoresis (current + treprostinil). From the first day of  
48 ulceration (D0) to complete re-epithelialization, treatments were applied daily, five days a  
49 week, during 20 minutes using a 100 µA cathodal continuous current, as previously  
50 described[3,10].  
51  
52  
53  
54  
55

### 56 *Assessment of wound healing*

1 Wound healing was quantified daily from photographs taken with a digital camera and  
2 an internal standard for size calibration. Blinded analyses of wound surface were realized with  
3 ImageJ software (National Institutes of Health, Bethesda, Maryland, USA). Wound healing was  
4 estimated by measuring the wound area (mm<sup>2</sup>). Then, wound area was expressed in percent  
5 change from the initial wound area measured on D0 (%BL). Areas under the curve (AUC) of  
6 wound healing rate over time were subsequently calculated.  
7  
8  
9

### 10 *Assessment of microvascular reactivity*

11 Endothelial and non-endothelial skin microvascular reactivity were explored at baseline  
12 (to validate the models) and after re-epithelialization (to assess the effect of treprostinil  
13 iontophoresis) using iontophoresis of acetylcholine (Ach) and sodium nitroprusside (SNP),  
14 respectively. Details about iontophoresis protocols are available in online supplementary  
15 methods.  
16  
17  
18  
19  
20  
21  
22

### 23 *Tissue histology*

24 Skin tissue samples, obtained at wound induction and after complete re-  
25 epithelialization, were fixed and paraffin-embedded. Samples were stained and examined by a  
26 dermatopathologist blinded to the group. Inflammatory infiltrate (macrophages), microvessel  
27 density, and collagen deposition and distribution were rated semi-quantitatively. More details  
28 regarding the histology protocol and the analysis are provided as online supplementary  
29 methods.  
30  
31  
32  
33  
34  
35  
36  
37  
38

## 39 **RESULTS**

### 40 *Validation of a mouse model of SSc-related delayed wound healing*

41 We observed no significant difference in wound healing between HOCl mice and their  
42 controls (AUC were 345±54 vs 418±85 %D0.day, respectively; p=0.112) (Figure S1).  
43 Secondary analyses focused on the first five days of wound healing as a *post hoc* exploration,  
44 to see whether the observed overall changes were retrieved during the early phase (week 1).  
45 Again, HOCl mice did not exhibit reduced wound healing in comparison with controls (AUC  
46 were -18±20, vs 4±27 %D0.day, respectively; p=0.14) (Figure S1). There were significant  
47 differences in cutaneous microvascular reactivity at baseline between HOCl mice and their  
48 controls in response to SNP (47 [40–65] vs 102 [70–141], respectively; p=0.011) and to Ach  
49 (25 [22–46] vs 50 [39–53], respectively; p=0.043) (Figure S2). However, macroscopic  
50 evaluation of the skin showed only limited fibrosis, associated with necrosis.  
51  
52  
53  
54  
55  
56  
57  
58  
59  
60

1 On the other hand, uPAR<sup>-/-</sup> mice exhibited reduced wound healing over time compared  
2 with controls (AUC were 468±97 vs 573±59 %D0.day, respectively; p=0.001) (Figure 1; Figure  
3 S3). We observed no significant difference in wound healing between female and male  
4 (541±106 vs 495±80 %D0.day, respectively; p=0.124). The sex\*genotype interaction was not  
5 significant (p=0.68), suggesting comparable impairment in wound healing between male and  
6 female uPAR<sup>-/-</sup> mice. Results over the first five days of treatment were comparable, with  
7 impaired wound healing in uPAR<sup>-/-</sup> vs controls (-1±33, vs 25±32, %D0.day, respectively;  
8 p=0.045), with no significant difference between female and male (19 ± 36 vs 3 ± 32 %D0,  
9 respectively; p=0.223) (Figure 1), and no sex\*genotype interaction (p=0.971). There was a  
10 significant difference in cutaneous microvascular reactivity at baseline between uPAR<sup>-/-</sup> mice  
11 and their controls, in response to ACh (17 [14 – 34] vs 49 [26 – 72] %BL, respectively; p=0.02)  
12 but not to SNP (48 [34–79] vs 63 [27–86] %BL, respectively; p=0.844) (Figure S4). We  
13 observed no significant difference in microvessel, macrophage or collagen density on  
14 histological analyses, although the latter tended to be decreased in uPAR<sup>-/-</sup> mice (p=0.06)  
15 (Table S1).

16 We thus retained the uPAR<sup>-/-</sup> model, and combined males and females to assess the  
17 effect of the treatment on wound healing in the following experiments.

### 18 *Treprostinil iontophoresis enhances wound healing in uPAR<sup>-/-</sup> mice*

19 In uPAR<sup>-/-</sup> mice, iontophoresis of treprostinil significantly improved wound healing  
20 (AUC were 591±53 %D0.day for treprostinil, 487±99 %D0.day for ES, and 468±97 %D0.day  
21 for the untreated group; p=0.002) (Figure 2; Figure S5). Adjusted paired comparisons showed  
22 that treprostinil was significantly superior to both ES and untreated groups (p=0.002 and  
23 p=0.030, respectively), while these two did not differ in a significant way (p=1.0) (Figure 2).

24 During the first five days, *post hoc* exploration yielded similar results (AUC were 52±20  
25 %D0.day for treprostinil, 12±41 %D0.day for ES, and -1 ± 33 %D0.day for the untreated group;  
26 p<0.001) with significant differences between treprostinil and ES or untreated groups  
27 (p=0.002), while these two did not differ (p=1.0) (Figure 2).

### 28 *Effect of treprostinil iontophoresis on inflammation, microvascular density and collagen*

29 Inflammatory infiltrate in re-epithelialized skin was decreased in the treprostinil group  
30 in comparison with both ES and untreated groups (Table S2). Iontophoresis of treprostinil  
31 increased microvessel density when compared to the untreated site (p<0.05), but the difference



was no longer significant when compared with ES (Table S2). Finally, we did not observe any difference between groups regarding collagen deposition and distribution (Table S2).

### *Effect of treprostinil iontophoresis on cutaneous vascular reactivity*

After complete re-epithelialization, we observed no significant difference between treprostinil iontophoresis, ES, or untreated skin, neither for Ach (33 [21–51], n=4; 37 [17–51], n=4; 26 [18–74], n=5; p=0.98) nor for SNP reactivity tests (62 [54–68], n=4; 53 [40–67], n=4; 66 [62–91], n=5; p=0.29)).

## DISCUSSION

In this study, we investigated the effect of an original pharmacological approach to enhance cutaneous wound healing in a mouse model of scleroderma-related ulcers. We first developed a model of SSc-related ulcers, using two mouse models known to have impaired vascular function. Since we did not succeed to reproduce the fibrosis phenotype of HOCl chemically-induced SSc [8], and because of a lack of significant delay in wound healing and a frequent occurrence of tissue necrosis, we did not retain this model. On the other hand, uPAR<sup>-/-</sup> mice presented impaired wound healing, associated with decreased response to acetylcholine iontophoresis, which suggests an impairment of endothelium-dependent vasodilation. This finding is consistent with previous work showing that microvascular endothelial cells from systemic sclerosis patients actually expressed a truncated uPAR protein, which appeared to be involved in the vascular pathophysiological mechanism of SSc[11].

Our main results suggest that iontophoresis of treprostinil can accelerate re-epithelialization of excisional ulcers in uPAR<sup>-/-</sup> mice. Of note, this effect does not seem to be associated with improved endothelium-dependent microvascular reactivity, although we only had a small number of animals and may have lacked of power. In contrast, we observed decreased inflammation in re-epithelialized skin after treprostinil iontophoresis. Since inflammation has a major impact on the early phase of wound healing, we conducted *post hoc* analyses on the effect of treprostinil on wound healing over the first five days of treatments, and confirmed that treatment effect was higher during this early phase.

Beyond the role of the prostacyclin pathway in vasodilation and inflammation, other pharmacological properties of treprostinil could be involved[12]. A study conducted in prostacyclin receptor (IP)-deficient mice showed decreased VEGF and angiogenesis during wound healing[13] while another prostacyclin analogue, iloprost showed vascular-protective effects on human SSc endothelial cells[14]. Thus, the positive effect of treprostinil could be associated with improved angiogenesis. This is consistent with the increased cutaneous

1  
2  
3  
4  
5  
6  
7  
8  
9  
10  
11  
12  
13  
14  
15  
16  
17  
18  
19  
20  
21  
22  
23  
24  
25  
26  
27  
28  
29  
30  
31  
32  
33  
34  
35  
36  
37  
38  
39  
40  
41  
42  
43  
44  
45  
46  
47  
48  
49  
50  
51  
52  
53  
54  
55  
56  
57  
58  
59  
60

microvessel density we observed after treatment. Yet, this effect may at least partly be attributed to the current itself, which has pro-angiogenic properties[10].

Although ES has been shown to enhance healing of chronic wounds in humans under certain conditions of intensity, polarity, and signal[6], the effect of ES on angiogenesis did not translate into accelerated wound healing in the present study. This suggests a potentiation between electrical and pharmacological responses on wound closure, since cathodal current is known to induce a PGI<sub>2</sub>-dependent vasodilation[15]. However, a limitation of this preliminary study is that it did not deeply explore the mechanisms underlying the effect of the intervention, and further work is needed explore the respective roles of prostacyclin endogenous synthesis induced by cathodal current and the exogenous IP activation by treprostinil.

In conclusion, excisional wounds in uPAR<sup>-/-</sup> mice appear to be a relevant model of SSc-related ulcers. Using this model, we show that iontophoresis of treprostinil, but not electrostimulation alone, improves wound healing. This effect is observed early, within the first five days of treatment, and is associated with enhanced angiogenesis and decreased inflammation. These results support the relevance of trials assessing the effect of iontophoresis of treprostinil on wound healing in patients with SSc-related digital ulcers.

#### RHEUMATOLOGY KEY MESSAGES

- Excisional wounds in uPAR<sup>-/-</sup> mice appear to be a relevant model of systemic sclerosis related ulcers.
- Treprostinil iontophoresis enhances wound healing in uPAR<sup>-/-</sup> mice.

#### FUNDING STATEMENT

This work was supported by the « Association des Sclérodermiques de France » and by the « Région Auvergne-Rhône-Alpes » (ARC programme).

#### ACKNOWLEDGMENTS

We warmly thank Prof. Meuth (Munster University, Germany) who graciously provided us with uPAR<sup>-/-</sup> mice.

#### CONFLICTS OF INTEREST

S. BLAISE, JL. CRACOWSKI and M. ROUSTIT declare a patent concerning the device using treprostinil (Remodulin®) to treat cutaneous ulcers (PCT/EP2014/065093).

## REFERENCES

- 1 Steen V, Denton CP, Pope JE, *et al.* Digital ulcers: overt vascular disease in systemic sclerosis. *Rheumatol Oxf Engl* 2009;48 Suppl 3:iii19-24. doi:10.1093/rheumatology/kep105
- 2 Kowal-Bielecka O, Fransen J, Avouac J, *et al.* Update of EULAR recommendations for the treatment of systemic sclerosis. *Ann Rheum Dis* 2017;76:1327-39. doi:10.1136/annrheumdis-2016-209909
- 3 Blaise S, Roustit M, Millet C, *et al.* Cathodal iontophoresis of treprostinil and iloprost induces a sustained increase in cutaneous flux in rats. *Br J Pharmacol* 2011;162:557-65. doi:10.1111/j.1476-5381.2010.01045.x
- 4 Roustit M, Gaillard-Bigot F, Blaise S, *et al.* Cutaneous iontophoresis of treprostinil in systemic sclerosis: a proof-of-concept study. *Clin Pharmacol Ther* 2014;95:439-45. doi:10.1038/clpt.2013.255
- 5 Zhao M, Song B, Pu J, *et al.* Electrical signals control wound healing through phosphatidylinositol-3-OH kinase- $\gamma$  and PTEN. *Nature* 2006;442:457-60. doi:10.1038/nature04925
- 6 Khouri C, Kotzki S, Roustit M, *et al.* Hierarchical evaluation of electrical stimulation protocols for chronic wound healing: An effect size meta-analysis: Electrical stimulation for wound healing. *Wound Repair Regen* 2017;25:883-91. doi:10.1111/wrr.12594
- 7 Guigui A, Mazet R, Blaise S, *et al.* Treprostinil Hydrogel Iontophoresis in Systemic Sclerosis-Related Digital Skin Ulcers: A Safety Study. *J Clin Pharmacol* 2020;60:758-67. doi:10.1002/jcph.1574
- 8 Servettaz A, Goulvestre C, Kavian N, *et al.* Selective Oxidation of DNA Topoisomerase 1 Induces Systemic Sclerosis in the Mouse. *J Immunol* 2009;182:5855-64. doi:10.4049/jimmunol.0803705
- 9 Manetti M, Rosa I, Milia AF, *et al.* Inactivation of urokinase-type plasminogen activator receptor (uPAR) gene induces dermal and pulmonary fibrosis and peripheral microvasculopathy in mice: a new model of experimental scleroderma? *Ann Rheum Dis* 2014;73:1700-9. doi:10.1136/annrheumdis-2013-203706
- 10 Bai H, McCaig CD, Forrester JV, *et al.* DC Electric Fields Induce Distinct Preangiogenic Responses in Microvascular and Macrovascular Cells. *Arterioscler Thromb Vasc Biol* 2004;24:1234-9. doi:10.1161/01.ATV.0000131265.76828.8a
- 11 Margheri F, Manetti M, Serrati S, *et al.* Domain 1 of the urokinase-type plasminogen activator receptor is required for its morphologic and functional, beta2 integrin-mediated connection with actin cytoskeleton in human microvascular endothelial cells: failure of association in systemic sclerosis endothelial cells. *Arthritis Rheum* 2006;54:3926-38. doi:10.1002/art.22263
- 12 Pluchart H, Khouri C, Blaise S, *et al.* Targeting the Prostacyclin Pathway: Beyond Pulmonary Arterial Hypertension. *Trends Pharmacol Sci* 2017;38:512-23. doi:10.1016/j.tips.2017.03.003
- 13 Manieri NA, Mack MR, Himmelrich MD, *et al.* Mucosally transplanted mesenchymal stem cells stimulate intestinal healing by promoting angiogenesis. *J Clin Invest* 2015;125:3606-18. doi:10.1172/JCI81423

- 1  
2  
3  
4  
5  
6  
7  
8  
9  
10  
11  
12  
13  
14  
15  
16  
17  
18  
19  
20  
21  
22  
23  
24  
25  
26  
27  
28  
29  
30  
31  
32  
33  
34  
35  
36  
37  
38  
39  
40  
41  
42  
43  
44  
45  
46  
47  
48  
49  
50  
51  
52  
53  
54  
55  
56  
57  
58  
59  
60
- 14 Tsou P-S, Palisoc PJ, Flavahan NA, *et al.* Dissecting the Cellular Mechanism of Prostacyclin Analog Iloprost in Reversing Vascular Dysfunction in Scleroderma. *Arthritis Rheumatol Hoboken NJ* 2021;73:520–9. doi:10.1002/art.41536
- 15 Gohin S, Sigaudou-Roussel D, Conjard-Duplany A, *et al.* What Can Current Stimulation Tell Us about the Vascular Function of Endogenous Prostacyclin in Healthy Rat Skin In Vivo? *J Invest Dermatol* 2011;131:237–44. doi:10.1038/jid.2010.267

For Peer Review

**FIGURE LEGENDS**

1  
2  
3  
4  
5 Figure 1. Wound healing after an excisional ulcer in uPAR<sup>-/-</sup> mice (n=8 males and 8 females) and their  
6 wild type littermates (uPAR<sup>+/+</sup>) (n=7 males and 8 females), over 5 days (panel A) and over 11 days  
7  
8 (panel B).  
9  
10  
11  
12  
13  
14

15 Figure 2. Effect of treprostinil iontophoresis (n=15) vs electro-stimulation (n=15) and untreated  
16 control (n=16) on wound healing, over 5 days (panel A) and over 11 days (panel B).  
17  
18  
19  
20  
21  
22  
23  
24  
25  
26  
27  
28  
29  
30  
31  
32  
33  
34  
35  
36  
37  
38  
39  
40  
41  
42  
43  
44  
45  
46  
47  
48  
49  
50  
51  
52  
53  
54  
55  
56  
57  
58  
59  
60

For Peer Review

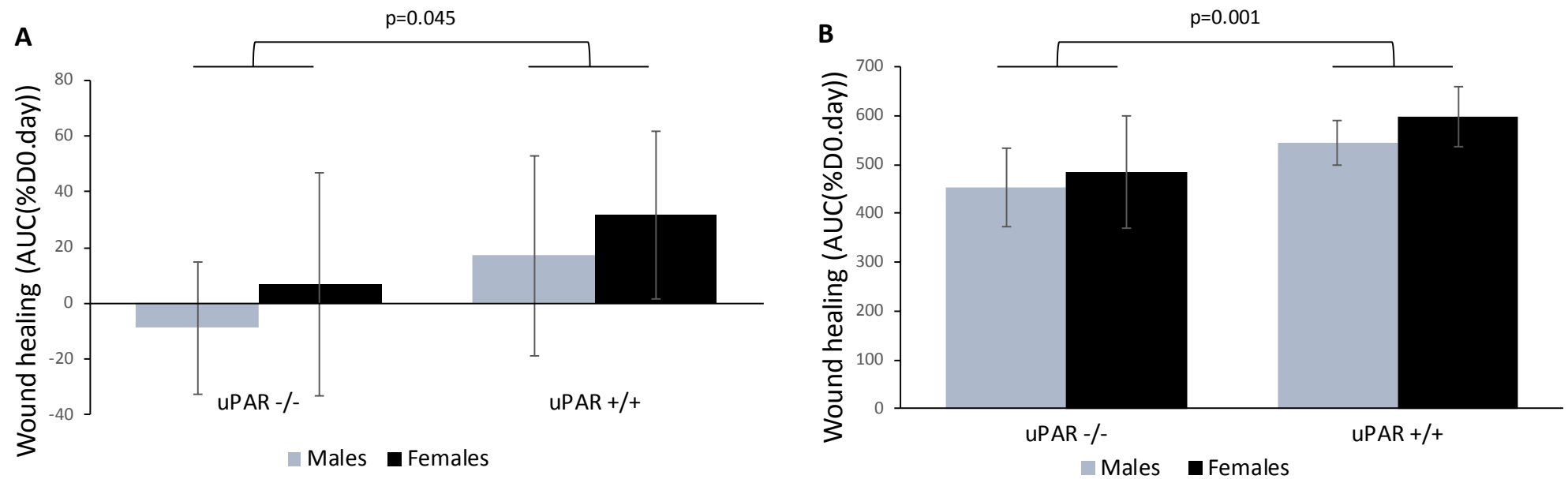


Figure 1. Wound healing after an excisional ulcer in uPAR<sup>-/-</sup> mice (n=8 males and 8 females) and their wild type littermates (uPAR<sup>+/+</sup>) (n=7 males and 8 females), over 5 days (panel A) and over 11 days (panel B).

1  
2  
3  
4  
5  
6  
7  
8  
9  
10  
11  
12  
13  
14  
15  
16  
17  
18  
19  
20  
21  
22  
23  
24  
25  
26  
27  
28  
29  
30  
31  
32  
33  
34  
35  
36  
37  
38  
39  
40  
41  
42  
43  
44  
45  
46

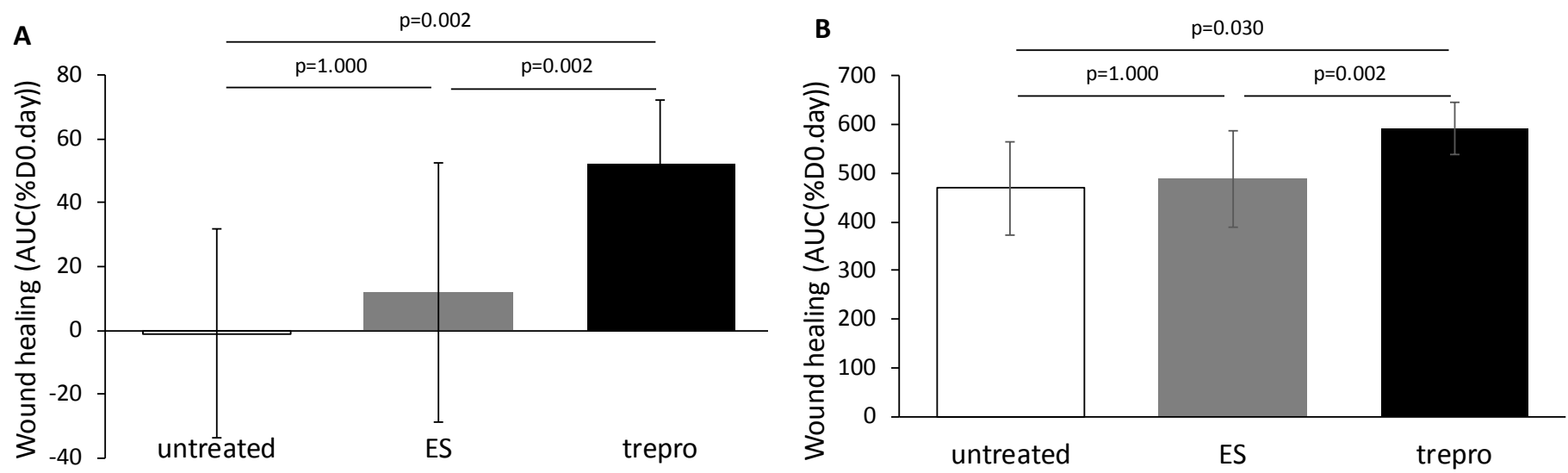


Figure 2. Effect of treprostinil iontophoresis (n=15) vs electro-stimulation (n=15) and untreated control (n=16) on wound healing, over 5 days (panel A) and over 11 days (panel B).

# Iontophoresis of treprostinil promotes wound healing in a murine model of scleroderma-related ulcers.

Sylvain KOTZKI\*, Yann SAVINA\*, Raphael BOUVET, Hugo GIL, Sophie BLAISE, Jean-Luc CRACOWSKI, Matthieu ROUSTIT

## Supplementary material

### Content

|  |    |
|--|----|
| Supplementary data .....   | 2  |
| Supplementary data S1 : Animal models.....   | 2  |
| Supplementary data S2 : uPAR DNA sequence .....  | 2  |
| Supplementary data S3 : Excisional wound model.....  | 3  |
| Supplementary data S4 : Assessment of microvascular reactivity .....   | 3  |
| Supplementary data S5 : Histological analysis .....  | 4  |
| Supplementary data S6 : Statistical analysis .....   | 5  |
| Supplementary tables .....   | 6  |
| Supplementary Table S1. Histological data of unwounded skin (baseline) and re-epithelialized skin according to mice genotype. ....   | 6  |
| Supplementary Table S2. Histological analysis of the cutaneous inflammatory infiltrate, microvascular density and collagen deposition after re-epithelialization.....  | 6  |
| Supplementary figures .....  | 7  |
| Supplementary Figure S1. Wound healing after an excisional ulcer in HOCl mice (n=7) and their controls (n=7), over 5 days (panel A) and over 11 days (panel B) .....   | 7  |
| Supplementary Figure S2. Skin microvascular response to iontophoresis of Ach and SNP in HOCl mice (Ach n=8, SNP n=7) in comparison with their controls (Ach n=9, SNP n=10). Data are expressed as median [1 <sup>st</sup> -3 <sup>rd</sup> quartiles] of the percent change from baseline of skin microvascular blood flux.....                      | 7  |
| Supplementary Figure S3. Kinetics of wound healing after an excisional ulcer in uPAR <sup>-/-</sup> mice (n=16) and their wild-type littermates (uPAR <sup>+/+</sup> ) (n=15), over 11 days, expressed as the daily percent change in wound area from baseline (D0). ....  | 8  |
| Supplementary Figure S4. Skin microvascular response to iontophoresis of Ach and SNP in uPAR <sup>-/-</sup> mice (Ach n=10, SNP n=8) in comparison with uPAR <sup>+/+</sup> mice (n=5 per group). Data are expressed as median [1 <sup>st</sup> -3 <sup>rd</sup> quartiles] of the percent change from baseline of skin microvascular blood flux.... | 8  |
| Supplementary Figure S5. Effect of treprostinil iontophoresis (n=15) vs NaCl iontophoresis (n=15) and untreated (n=16) on wound healing in uPAR <sup>-/-</sup> mice, over 11 days, expressed as the daily percent change in wound area from baseline (D0). ....  | 9  |
| References.....  | 10 |



## Supplementary data

### Supplementary data S1 : Animal models

#### Chemically-induced model (HOCl)

Seven-week-old female BALB/c mice (CERJ, Le Genest-Saint-Isle, France) were randomly distributed into HOCl and control groups (n=7 per group). Animals in the HOCl group received two dorsal intradermal injections of 250  $\mu$ l of hypochlorous acid (HOCl) daily during the first five days to generate oxidative stress. Then animals received one daily intradermal injection of 200  $\mu$ l of the same solution, five days a week during the next 5 weeks, as previously described[8]. The control group received injections of sterilized phosphate buffered saline (PBS) solution following the same protocol.

#### Genetic model (uPAR<sup>-/-</sup>)

The Urokinase-type Plasminogen Activator Receptor gene (uPAR<sup>-/-</sup>) mouse model mimics the vascular and fibrotic features of SSc[9]. uPAR<sup>-/-</sup> mice were crossed with wild-type (uPAR<sup>+/+</sup>) mice on a C57BL/6J background to generate heterozygous uPAR<sup>+/-</sup> mice. The latter were subsequently crossed to generate uPAR<sup>-/-</sup> and their uPAR<sup>+/+</sup> littermates as controls. PCR of tail-tip genomic DNA was performed to determine the absence or presence of a functional uPAR gene. Sixty-three male and female 12-week old mice (46 uPAR<sup>-/-</sup> and 17 uPAR<sup>+/+</sup>) were used from our breeding.

### Supplementary data S2 : uPAR DNA sequence

PCR of tail-tip genomic DNA was performed to determine the absence or presence of a functional uPAR gene using 3 primers sequences:

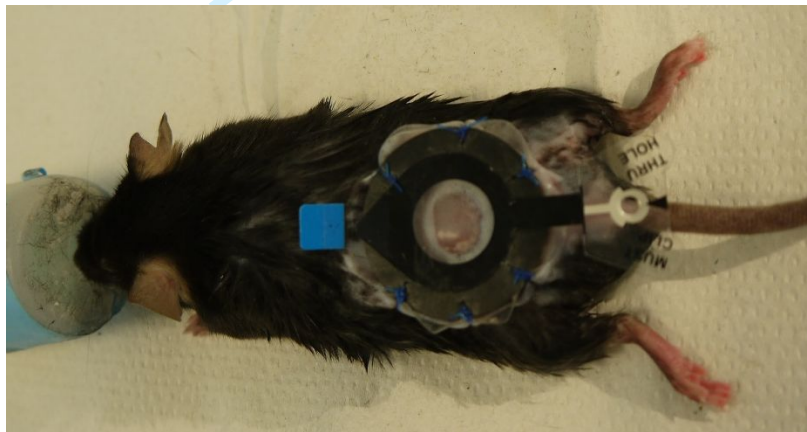
|             |                                 |
|-------------|---------------------------------|
| uPAR commun | AGAGCTCCGGTTCTCTCTC             |
| uPAR KO     | TATTACCAGTGAATCTTTGTCAGCAGTTCCC |
| uPAR WT     | GGGAGGAAGGAACTCCACTC            |

### Supplementary data S3 : Excisional wound model

Mice were anesthetized with isoflurane with a 3-min induction phase at 3% and a maintenance phase at 1.5%. Before wounding, analgesia was induced with buprenorphin at 0.1 mg/kg (intraperitoneal injection). The dorsal part of each mouse was shaved and a full-thickness skin excision wound extending through the panniculus carnosus was performed on the dorsal midline, with a sterile 6-mm biopsy punch.

A rubber ring (20/27 mm) was centered and fixed around the wound with a bi-component epoxy glue, and secured with interrupted 3/0 nylon sutures as previously described (1).

Rubber ring splinting was used to minimize wound contraction (2). Synthetic epoxy resin was applied to the perimeter of the rubber ring to improve adhesion to the skin and to protect it from mice bites, as shown on the picture below.



*Excisional wound model*

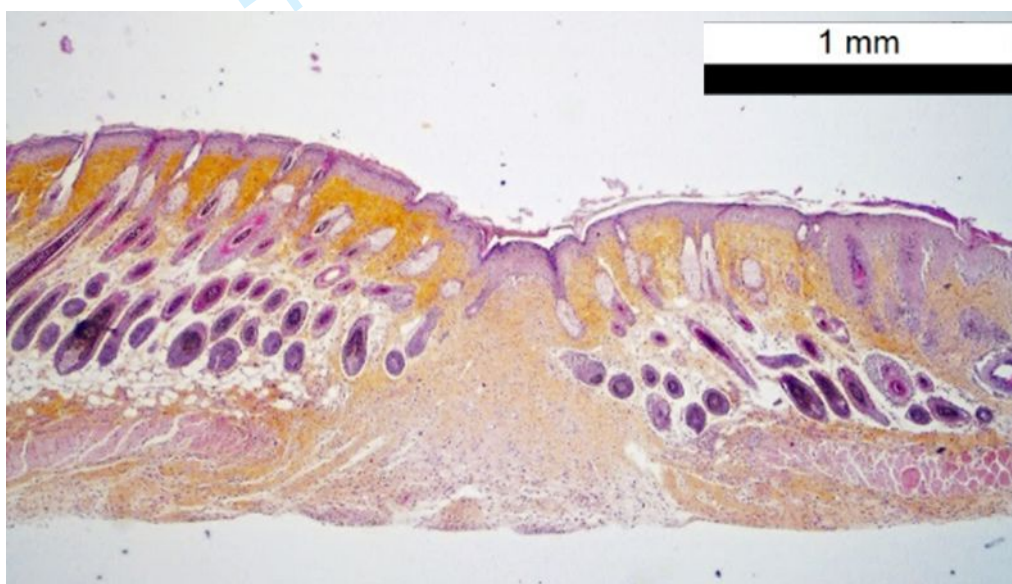
### Supplementary data S4 : Assessment of microvascular reactivity

Endothelial and non-endothelial skin microvascular reactivity were explored at baseline (to validate the models) and after re-epithelialization (to assess the effect of treprostinil iontophoresis). Skin blood flow was continuously recorded using laser Doppler Imaging (PIM3, Perimed, Järfälla, Sweden) before and during iontophoresis of vasodilators on the hairless back, using a 1.2 cm<sup>2</sup> electrode. Endothelium-dependent function was assessed using iontophoresis of acetylcholine (ACh) at 20 mg/mL (Sigma, Saint Quentin Fallavier, France) with a 100  $\mu$ A anodal current during 10 min. Endothelium-independent function was assessed using iontophoresis sodium nitroprusside (SNP) at 20 mg/mL (Nitriate; SERB, Paris, France) with a 100  $\mu$ A cathodal current during 10 min. Data were digitized, stored on a computer, and analysed offline with signal processing software (PimSoft

v1.5.4.8078, Perimed, Järfälla, Sweden). Baselines were expressed as arbitrary perfusion units (APUs) and vasodilatory responses as a percent change from baseline (%BL). The iontophoretic dose is defined as current multiplied by time of application  $\text{Dose } (\mu\text{A}\cdot\text{second}) = \text{current } (\mu\text{A}) \times \text{time (seconds)}$ , and the amount of drug delivered is directly proportional to the iontophoretic dose applied.

### Supplementary data S5 : Histological analysis

Biopsy were harvested and fixed in 4% formalin during 24 hours. After imbedding in a paraffin block, five-micrometer thickness sections were cut and hematoxylin, eosin and safran staining (Leica Autostainer XL, LeicaBiosystems, Wetzlar, Germany) was performed to evaluate morphological characteristics of the epidermis, dermis and hypodermis regions.



All samples were examined by a dermatopathologist blinded to the group, using an optical microscope (Olympus BX51, Tokyo, Japan). Microvessel density, collagen deposition and distribution, as well as inflammatory infiltrates (macrophages) were evaluated before wounding (baseline) and after complete re-epithelialization.

Microvascular density was quantified by counting the number of microvessels per high power field (400x magnification, diameter of field of view=0.62 mm), by differentiating new blood vessels, which are tufted and have turgescient endothelial lining, from pre-existing vessels.

The density of the inflammatory infiltrate was graded semi-quantitatively, as follows: 1, no inflammation; 2, discreet inflammation; 3, moderate inflammation; and 4, intense inflammation.

1  
2  
3 Collagen deposition and its distribution were evaluated using a microscope with polarised light  
4 (Olympus U-POT, Tokyo, Japan). Four groups were identified: 0, well organized collagen bundles; 1,  
5 disorganized and organized bundles; 2, disorganized fine fibres; and 3, no refringence.  
6  
7  
8  
9  
10  
11  
12  
13  
14

### 15 **Supplementary data S6 : Statistical analysis**

16  
17 Data were expressed as mean  $\pm$  standard deviation, or as median [1<sup>st</sup>-3<sup>rd</sup> quartiles] when  
18 not normally distributed. Wound healing was analysed using general linear models. To validate  
19 the mouse-model and assess whether sex has an influence, genotype and sex were used as fixed  
20 factors, and the genotype\*sex interaction was included in the model. The effect of treprostinil  
21 iontophoresis was assessed by including the treatment effect as a fixed factor. To take into  
22 consideration wound area at baseline, the latter was introduced as a covariate in all models.  
23 Non-normally distributed data were transformed. The Bonferroni method was used to account  
24 for multiple comparisons. Histological and vascular reactivity data were evaluated using non-  
25 parametric tests. A p-value of 0.05 or less was considered statistically significant. Statistical  
26 analyses were performed using SPSS 21.0 for Windows (IBM, SPSS, Chicago, IL).  
27  
28  
29  
30  
31  
32  
33  
34  
35  
36  
37  
38  
39  
40  
41  
42  
43  
44  
45  
46  
47  
48  
49  
50  
51  
52  
53  
54  
55  
56  
57  
58  
59  
60

## Supplementary tables

**Supplementary Table S1. Histological data of unwounded skin (baseline) and re-epithelialized skin according to mice genotype.**

|                              |                                       | uPAR <sup>-/-</sup> |           | uPAR <sup>+/+</sup> |               | p-value |       |
|------------------------------|---------------------------------------|---------------------|-----------|---------------------|---------------|---------|-------|
|                              |                                       | Median (IQ)         | n         | Median (IQ)         | n             |         |       |
| Baseline (D0)                | Microvessels density <sup>#</sup>     | 3.0                 | [2.0-4.0] | 1.5                 | [1.0-2.0]     | 0.147   |       |
|                              | Inflammatory infiltrate <sup>##</sup> | 1.0                 | [1.0-1.0] | 5                   | 1.0 [1.0-1.0] | 8       | 1.000 |
|                              | Collagen <sup>###</sup>               | 0.0                 | [0.0-0.0] | 0.0                 | [0.0-0.0]     | 1.000   |       |
| Re-epithelialized skin (D11) | Microvessels density                  | 1.0                 | [1.0-1.5] | 8                   | 1.0 [1.0-1.0] | 11      | 0.324 |
|                              | Inflammatory infiltrate               | 1.0                 | [0.5-1.5] | 9                   | 1.0 [0.0-2.0] | 15      | 0.946 |
|                              | Collagen                              | 0.0                 | [0.0-0.0] | 9                   | 0.0 [0.0-0.0] | 14      | 1.000 |

Data are expressed as median [1<sup>st</sup>-3<sup>rd</sup> quartiles] scores. <sup>#</sup>number of microvessels per high power field, <sup>##</sup> semi-quantitative analysis <sup>###</sup>0, well organized collagen bundles; 1, disorganized and organized bundles; 2, disorganized fine fibres; and 3, no refringence

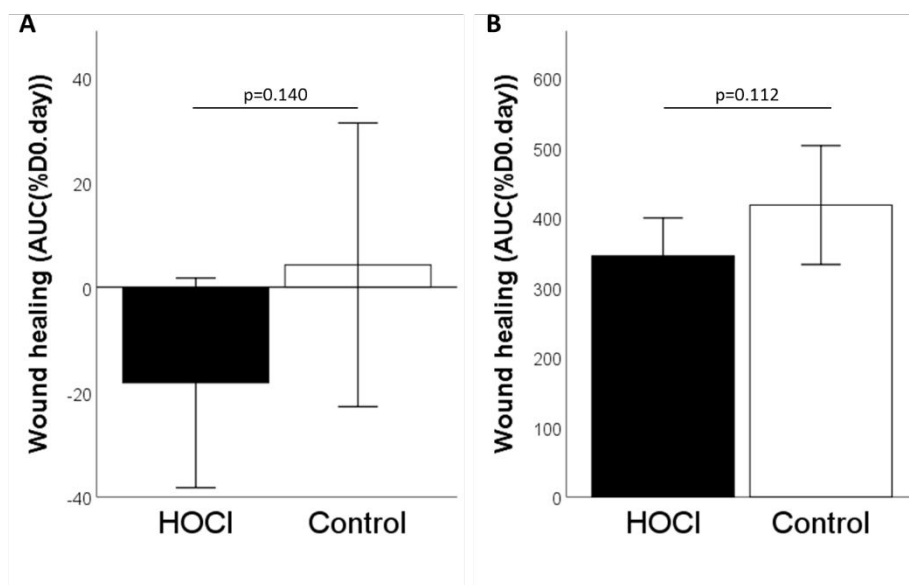
**Supplementary Table S2. Histological analysis of the cutaneous inflammatory infiltrate, microvascular density and collagen deposition after re-epithelialization.**

|                                       | untreated   |           |   | NaCl        |            |   | treprostiniil     |           |    | p-value |
|---------------------------------------|-------------|-----------|---|-------------|------------|---|-------------------|-----------|----|---------|
|                                       | Median (IQ) | n         |   | Median (IQ) | n          |   | Median (IQ)       | n         |    |         |
| Microvessels density <sup>#</sup>     | 1.0         | [1.0-1.0] | 7 | 1.0         | [1.0-2.0]  | 6 | 2.0*              | [1.0-3.0] | 10 | 0.039   |
| Inflammatory infiltrate <sup>##</sup> | 1.0         | [1.0-1.5] | 7 | 1.0         | [0.0-2.00] | 6 | 0.0* <sup>§</sup> | [0.0-1.0] | 10 | 0.029   |
| Collagen <sup>###</sup>               | 0.0         | [0.0-0.0] | 7 | 0.0         | [0.0-0.0]  | 6 | 0.0               | [0.0-0.0] | 10 | 1.000   |

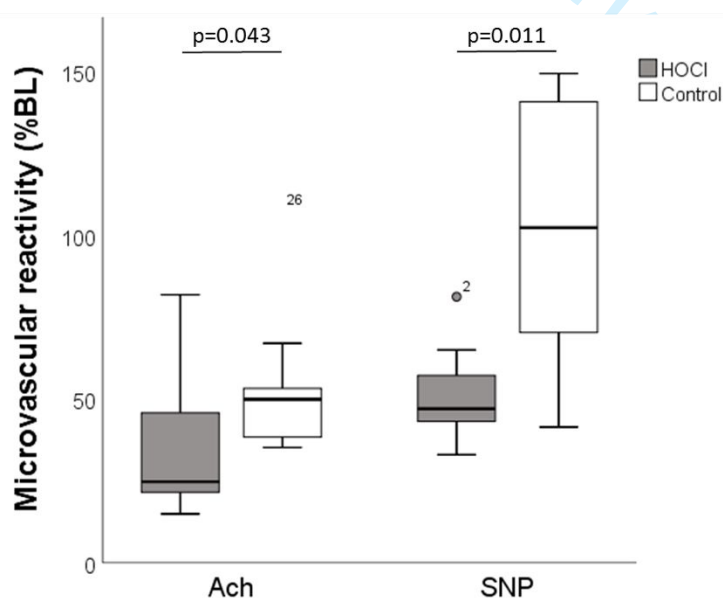
Data are expressed as median [1<sup>st</sup>-3<sup>rd</sup> quartiles] scores. Significance: \*p<0.05 vs untreated, <sup>§</sup>p<0.05 vs NaCl. <sup>#</sup>number of microvessels per high power field, <sup>##</sup> semi-quantitative analysis <sup>###</sup>0, well organized collagen bundles; 1, disorganized and organized bundles; 2, disorganized fine fibres; and 3, no refringence

## Supplementary figures

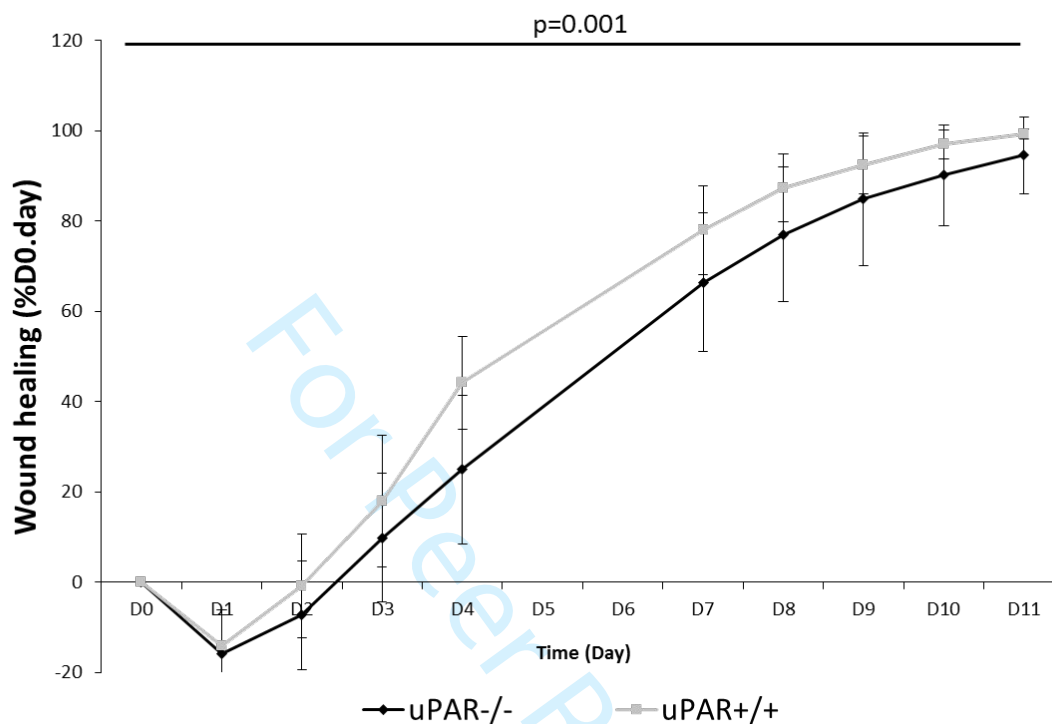
Supplementary Figure S1. Wound healing after an excisional ulcer in HOCl mice (n=7) and their controls (n=7), over 5 days (panel A) and over 11 days (panel B)



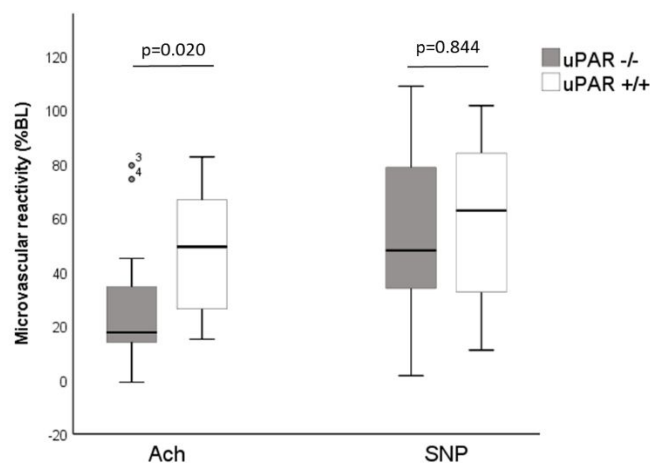
Supplementary Figure S2. Skin microvascular response to iontophoresis of Ach and SNP in HOCl mice (Ach n=8, SNP n=7) in comparison with their controls (Ach n=9, SNP n=10). Data are expressed as median [1<sup>st</sup>-3<sup>rd</sup> quartiles] of the percent change from baseline of skin microvascular blood flux.



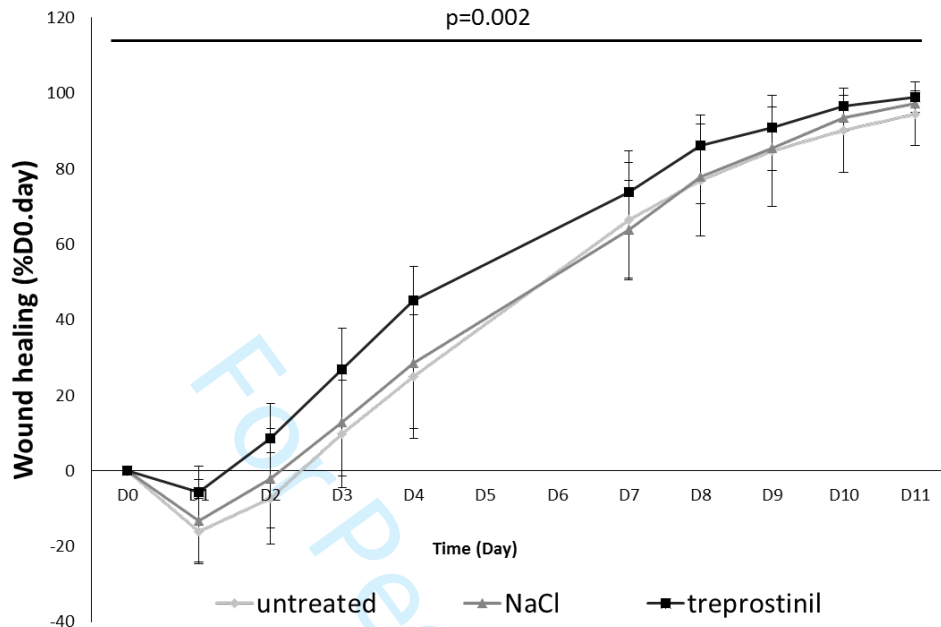
Supplementary Figure S3. Kinetics of wound healing after an excisional ulcer in  $uPAR^{-/-}$  mice (n=16) and their wild-type littermates ( $uPAR^{+/+}$ ) (n=15), over 11 days, expressed as the daily percent change in wound area from baseline (D0).



Supplementary Figure S4. Skin microvascular response to iontophoresis of Ach and SNP in  $uPAR^{-/-}$  mice (Ach n=10, SNP n=8) in comparison with  $uPAR^{+/+}$  mice (n=5 per group). Data are expressed as median [1st-3rd quartiles] of the percent change from baseline of skin microvascular blood flux.



Supplementary Figure S5. Effect of treprostinil iontophoresis (n=15) vs NaCl iontophoresis (n=15) and untreated (n=16) on wound healing in uPAR<sup>-/-</sup> mice, over 11 days, expressed as the daily percent change in wound area from baseline (D0).





## References

1. Galiano RD, Michaels V Joseph, Dobryansky M, Levine JP, Gurtner GC. Quantitative and reproducible murine model of excisional wound healing. *Wound Repair and Regeneration*. 1 août 2004;12(4):485-92.
2. Windsor ML, Eisenberg M, Gordon-Thomson C, Moore GP. A novel model of wound healing in the SCID mouse using a cultured human skin substitute. *Australasian Journal of Dermatology*. 1 févr 2009;50(1):29-35.

For Peer Review

1  
2  
3  
4  
5  
6  
7  
8  
9  
10  
11  
12  
13  
14  
15  
16  
17  
18  
19  
20  
21  
22  
23  
24  
25  
26  
27  
28  
29  
30  
31  
32  
33  
34  
35  
36  
37  
38  
39  
40  
41  
42  
43  
44  
45  
46  
47  
48  
49  
50  
51  
52  
53  
54  
55  
56  
57  
58  
59  
60